INFLUENCE OF Cu_2O DOPING ON CRYSTAL STRUCTURE AND THERMOELECTRIC PROPERTIES OF $CaMnO_3$

Kunchit Singsoog [a,b], Supasit Pangson [a], Panida Pilasuta [a], Wanachaporn Namhongsa [a], Urai Seetawan[c], Pennapa Muthitamongkol [d], Chanchana Thanachayanont [d] and Tosawat Seetawan [a,b*]

[a]*Program of Physics, Faculty of Science and Technology, Sakon Nakhon Rajabhat University, Sakon Nakhon, 47000, Thailand*
[b]*Thermoelectrics Research Center, Research and Development Institute, Sakon Nakhon Rajabhat University, Sakon Nakhon, 47000, Thailand*
[c]*Thatnaraiwittaya School, 606 Nittayo Rd., Sakon Nakon, 47000, Thailand*
[d]*The National Metals and Materials Technology Center Thailand Science Park, Pathumthani, 12120, Thailand*

Received 22 December 2014; Revised 15 April 2015; Accepted 15 April 2015

ABSTRACT

Doped thermoelectric materials can bring beneficial change to thermoelectric properties. The Cu_2O (5%, 10%, 15%, 20% and 25%) doped $CaMnO_3$ samples were synthesized by solid state reaction method. The samples analyzed by X-ray diffraction shows orthorhombic perovskite crystal structure. The crystallite size decreased with increasing doping content, which was confirmed by calculating from Scherrer's equation and reconfirmed through imagines of scanning electron microscope. Thermoelectric properties including Seebeck coefficient and electrical resistivity were measured in temperature range of 323 – 473 K. Cu_2O doping increased the Seebeck coefficient (except for doping content 25%) and decreased electrical resistivity. The Cu_2O doped $CaMnO_3$ samples all showed enhancement of thermoelectric properties. Doping with 5% Cu_2O had the maximum power factor of 86.8 $\mu W/m \cdot K^2$ at 473 K.

KEYWORDS: *Power factor, Thermoelectric properties, $CaMnO_3$, Cu_2O doped*

* Corresponding authors; e-mail: t_seetawan@snru.ac.th, Tel.&Fax +6642744319

INTRODUCTION

Thermoelectric materials continue to be developed for higher efficiencies. A good thermoelectric material should possess large power factor [1-3] ($PF=S^2/\rho$; PF is power factor, S is Seebeck coefficient and ρ is electrical resistivity).

$CaMnO_3$ is an n-type thermoelectric material and shows typical behavior of a semiconductor [4]. The crystal structure of the material is orthorhombic symmetry [2, 5-10]. The material has a large Seebeck coefficient (S ~ 460 μV/K at near room temperature) [11], which is interesting as a thermoelectric material. However, the $CaMnO_3$ obtained has high electrical resistivity [11, 12], which impacts poorly on the thermoelectric property. Such a problem can be solved by doping with higher valence elements. Dual-doped $Ca_{1-2x}Dy_xBi_xMnO_3$ had obtained electrical resistivity decrease continuously with increasing doping content [13]. The electrical resistivity of rare earth Pr doped $Ca_{1-x}Pr_xMnO_3$ was remarkably reduced with increasing doping concentration [12]. Although high valence element doping can reduce electrical resistivity, the Seebeck coefficient correspondingly reduces as well [7, 12, 13]. In this work, we attempted to reduce the electrical resistivity and increase the Seebeck coefficient of $CaMnO_3$ with Cu_2O doping by solid state reaction method to enhancement power factor.

MATERIALS AND METHODS

Powders of $CaCO_3$ and MnO_2 were used as raw materials for synthesis of $CaMnO_3$ doped with Cu_2O (5%, 10%, 15%, 20% and 25% by mol) by solid state reaction method. The powders were mixed by ball-milling and calcined at 1123 K for 10 h in ambient atmosphere. The calcined powder was ground with polyvinyl alcohol for 2 h. The products were pressed into pellets at 14.70 MPa

and sintered in ambient atmosphere condition at 1423 K for 36 h.

The crystal structure was characterized by X-ray diffractometer Shimazhu 6100 with CuKα radiation in angle range of 20-80°. The crystallite size was calculated by Scherrer's equation ($\beta_s = \lambda/d\cdot\cos\theta$; where β_s, λ, d and θ are full width at half maximum (FWHM), X-ray wavelength, crystallite size and diffraction angle, respectively). The density and hardness were measured by NewClassic Balances MS Semi-Micro Models and MicroVickers Hardness Tester Shimazhu, respectively. The microstructure was obtained from scanning electron microscope. The electrical resistivity and Seebeck coefficient were measured by steady state method together with calculated the power factor in temperature range of 323-473 K.

RESULTS AND DISCUSSION

The X-ray diffraction pattern at room temperature of Cu_2O doped $CaMnO_3$ are shown in Fig. 1. The diffraction peaks are indexed by comparing with ICDD PDF card number 01-078-3978 for orthorhombic Pnma symmetry. A small amount of mixed phase Cu_2O and CuO are found. The lattice parameter and unit cell volume increases with Cu_2O doped content as shown in Fig. 2 and Fig. 3, respectively.

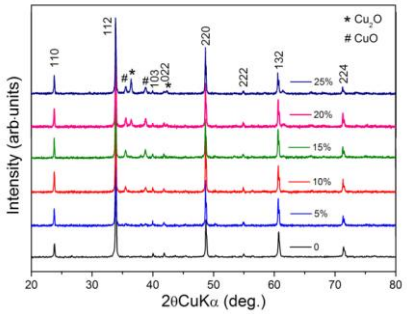

Fig. 1. X-ray diffraction pattern of Cu_2O doped (0, 5, 10, 15, 20 and 25%) $CaMnO_3$

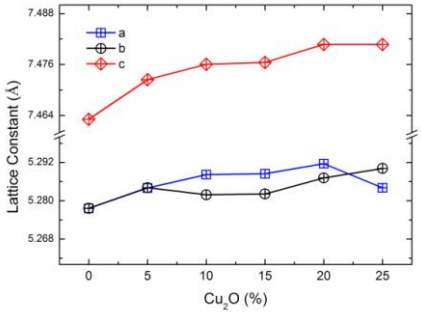

Fig. 2. Doping content dependence of the lattice constant

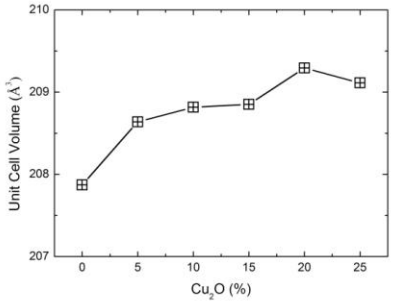

Fig. 3. Doping content dependence of the unit cell volume

The full width at half maximum (FWHM) of the diffraction peaks for Cu_2O doped $CaMnO_3$ tends to get slightly broader as the doping content increases, which indicates a decreasing crystallite size shown in Table 1. Furthermore, crystal size decreased with doping content can be observe from scanning electron microscope imagines as shown in Fig. 4, which is agreement with our estimation from FWHM by XRD. Measured densities are 3.626, 3.815, 3.959, 4.067 and 4.196 for sample with 5, 10, 15, 20 and 25% of Cu_2O doped, respectively. The measured density increases with an increase of doping content, mainly due to the contribution from the mass of Cu elements. The relative densities, defined as the measured density over the theoretical density, are all over 81% and up to 90.05% at 25% of Cu_2O doped as shown in Table 2.

Table 1. FWHM and crystallite size of Cu_2O doped (0, 5, 10, 15, 20 and 25%) $CaMnO_3$

Cu_2O doped (%)	FWHM	Crystallite size (μm)
5	0.1959±0.0005	1.02±0.08
10	0.1963±0.0009	0.80±0.06
15	0.1967±0.0012	0.79±0.26
20	0.2026±0.0035	0.46±0.18
25	0.2031±0.0024	0.45±0.16

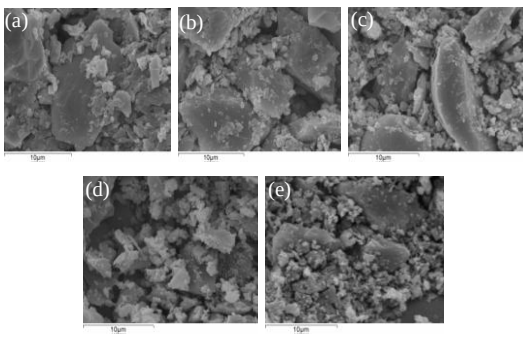

Fig. 4. SEM image of Cu_2O doping content (a) 5% (b) 10% (c) 15% (d) 20% and (e) 25%

Table. 2. Hardness and density of Cu_2 doped (0,5, 10, 15, 20 and 25%) $CaMnO_3$

Cu_2O doped (%)	Hardness (HV)	Theoretical Density (g/cm^3)	Density (g/cm^3)	Relative Density (%)
5	420	4.47	3.626	81.16
10	515	4.51	3.815	84.51
15	524	4.56	3.959	86.74
20	543	4.61	4.067	88.31
25	545	4.66	4.196	90.05

Fig. 5 shows the temperature dependence of the Seebeck coefficient for Cu_2O doped (0, 5, 10, 15, 20 and 25%) $CaMnO_3$ between 323 K and 473 K. The Seebeck coefficient are all negative, which confirms that the samples are n-type thermoelectric materials [14]. The absolute Seebeck coefficients of Cu_2O doped up to 20% are greater while doped 25% is less when compare with un-doped $CaMnO_3$. The trend of absolute Seebeck coefficient increases with doping content up to 15% and decreases as the doping content further increases as shown in the inset of Fig. 5.

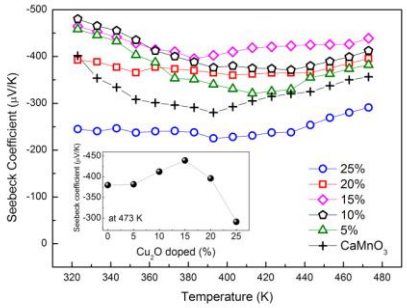

Fig. 5. Temperature dependence of the Seebeck coefficient for Cu_2O doped (0, 5, 10, 15, 20 and 25%) $CaMnO_3$

The measured electrical resistivity of $CaMnO_3$ doped with Cu_2O in temperature range 323 K – 473 K are shown in Fig. 6. The electrical resistivities of all samples decrease with increasing temperature, which is indicative that these samples show semiconductor behavior [3, 9]. The un-doped $CaMnO_3$ shows high electrical resistivity which decreases with increasing temperature and is in agreement with literature data [1, 2, 11, 12, 14] as shown in the inset in Fig. 6. The electrical resistivity of Cu_2O doped samples is lower than un-dope $CaMnO_3$ which could be explained by an increase in the electron carrier concentration [1, 4, 13]. The electrical resistivity of Cu_2O doped samples increase with doping content up to 15% and decrease as the doping content further increases. The trend of electrical resistivity with doping content corresponds with Seebeck coefficient trend. The electrical resistivity of doping content 5% shows the lowest value of 1.68 mΩ·m at 473 K.

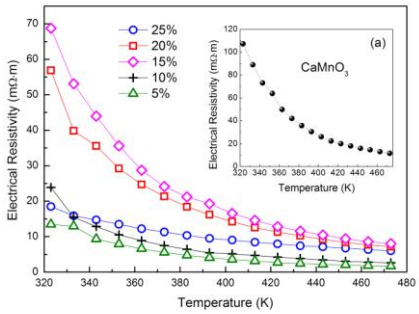

Fig. 6. Temperature dependence of the electrical resistivity for Cu_2O doped (0, 5, 10, 15, 20 and 25%) $CaMnO_3$

The most appropriate doping content can be obtained by analyzing the power factor as plotted with temperature in Fig. 7. The power factors of doped $CaMnO_3$ are higher than un-doped $CaMnO_3$ especially for doping contents of 5 and 10%. The power factor value for the un-doped sample is 2.086 μW/m·K^2 at 373 K, similar to the result reported by M. Mouyane et al. [11]. The Cu_2O 5% doped $CaMnO_3$ shows the highest power factor of 86.82 μW/m·K^2 at 473 K.

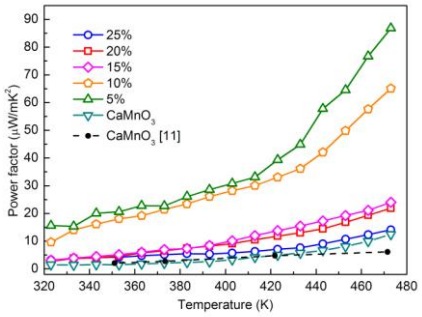

Fig. 7. Temperature dependence of the power factor for Cu_2O doped (0, 5, 10, 15, 20 and 25%) $CaMnO_3$

CONCLUSION

Cu_2O doped (0, 5, 10, 15, 20 and 25%) $CaMnO_3$ samples were successfully synthesized using solid state reaction method. The influence of Cu_2O doped $CaMnO_3$ is analyzed. It was found that, the lattice parameter and unit cell volume increased while crystallite size decreased as doping content increased. Also the Seebeck coefficient increased in all doping content (except for 25%). The electron carrier concentration increased, demonstrated by the decrease of electrical resistivity. The 5% Cu_2O doped $CaMnO_3$ shows the highest power factor.

ACKNOWLEDGEMENTS

This paper has been financially supported by the Electricity Generating Authority of Thailand (EGAT).

REFERENCES

[1] B. Zhan, J. Lan, Y. Liu, Y. Lin1, Y. Shen, C. Nan: *J. Mater. Sci. Technol*. **2014** 821-825.
[2] Y-H. Zhun, W-B. Su, J. Liu, Y-C. Zhou, J. Li, X. Zhang, Y. Du, C-L. Wang: *J. Ceram. Int.* **2015** 1535–1539.
[3] F.P. Zhang, Q.M. Lu, X. Zhang, J.X. Zhang: *J. Phys Chem Solids*. **2013** 1859–1864.
[4] J.W. Park, D.H. Kwak, S.H. Yoon, S.C. Choi : *J. Alloy Compd*. **2009** 550–555.
[5] A. Kompany, T. G. Moghadam, S. Kafash, M. E. Abrishami: Frequency dependence of Néel temperature in $CaMnO_{3-\delta}$ ceramics: Synthesized by two different methods.
[6] Q. Zhou, B. J. Kennedy: *J. Phys Chem Solids.* **2006** 1595–1598.
[7] A. Bhaskar, J.J. Yuan, C-J. Liu: *Mater Sci Eng B.* **2014** 48–53.
[8] R. Kabir, D. Wang, T. Zhang, R. Tian, R. Donelson, Th. T. Tan, S. Li *: Ceram Int*. **2014** 16701–16706.
[9] X.Y. Huang, Y. Miyazaki, T. Kajitani: *Solid State Communications.* **2008** 132–136.
[10] M.E. Melo Jorge, A. Correia dos Santos, M.R. Nunes: *Int J Inorg Mater*. **2001** 915–921.
[11] M. Mouyane, B. Itaalit, J. Bernard, D. Houivet, J. G. Noudem: *Powder Technol*. **2014** 71–77.
[12] Z. Feipeng, N. Baocheng, Z. Kunshu, Z. Xin, L. Qingmei and Z. Jiuxing: *J. Rate Earth.* **2013** 885-890.
[13] Y. Zhu, C. Wang, H. Wang, W. Su, J. Liu, J. Li: *Mater Chem Phys*. **2014** 385-389.
[14] E. I. Goldyreva, I. A. Leonidov, M. V. Patrakeev, V. L. Kozhevnikov: *Solid State Ionics.* **2014** 678–681.